Spectrally Efficient WDM Nyquist Pulse-Shaped 16-QAM Subcarrier Modulation Transmission With Direct Detection

M. Sezer Erkılınç, *Student Member, IEEE*, Zhe Li, *Student Member, IEEE*, Stephan Pachnicke, *Senior Member, IEEE*, Helmut Griesser, *Member, IEEE*, Benn C. Thomsen, *Member, IEEE*, Polina Bayvel, *Fellow, IEEE, Fellow, OSA*, and Robert I. Killey, *Member, IEEE*

***Abstract*—The ability to transmit signals with high information spectral density (ISD) using low-complexity and cost-effective transceivers is essential for short- and medium-haul optical communication systems. Consequently, spectrally efficient direct detection transceiver-based solutions are attractive for such applications. In this paper, we experimentally demonstrate the wavelength-division multiplexed (WDM) transmission of 7×12 GHz-spaced dispersion pre-compensated Nyquist pulse-shaped 16-QAM subcarrier modulated channels operating at a net bit rate of 24 Gb/s per channel, and achieving a net optical ISD of 2.0 b/s/Hz. The direct detection receiver used in our experiment consisted of a single-ended photodiode and a single analog-to-digital converter. The carrier-to-signal power ratio at different values of optical signal-to-noise ratio was optimized to maximize the receiver sensitivity performance. The transmission experiments were carried out using a recirculating fiber loop with uncompensated standard single-mode fiber and EDFA-only amplification. The maximum achieved transmission distances for single channel and WDM signals were 727 and 323 km below the bit-error ratio of 3.8×10^{-3}, respectively. To the best of our knowledge, this is the highest achieved ISD for WDM transmission in direct detection links over such distances.**

***Index Terms*—Digital signal processing, direct detection, information spectral density, Nyquist pulse shaping, optical fiber communication, single sideband signaling, subcarrier modulation, transceiver design, wavelength division multiplexing.**

I. Introduction

CONTINUOUSLY increasing high bandwidth demand due to data intensive services such as IP-TV, high-definition video-on-demand and cloud computing requires spectrally-efficient modulation formats in access, metropolitan and regional links [1], [2]. Multi-level and multi-dimensional modulation formats, e.g., quadrature amplitude modulation (QAM) with polarization multiplexing, using coherent receivers combined with digital signal processing (DSP)-based compensation of fiber impairments [3] enable the highest channel bit rates and information spectral densities (ISDs) [4], [5]. However, cost-effectiveness is another essential requirement for short- and medium-haul links ($\leq$800 km) in which direct detection (DD) might be favorable due to its lower optical complexity. Thus, DSP-enabled transceivers employing DD receivers, i.e., consisting of only a single-ended photodiode and a single analogue-to-digital converter (ADC), offer promising and practical solutions for metro and access links. Recently, service providers have started deploying 100 Gb/s metro solutions based on 4 × 28 Gb/s DD technology [6].

In this paper, we describe experimental demonstrations of single channel and WDM transmission (12 GHz-spaced seven channels) of single sideband (SSB) Nyquist pulse-shaped 16-QAM subcarrier modulated signals using DD. The receiver consisted of only a single-ended photodiode and a single ADC. Back-to-back and transmission performance was assessed at a net bit rate of 24 Gb/s per channel with a net optical ISD of 2.0 b/s/Hz (a gross bit rate of 25 Gb/s with a gross optical ISD of 2.08 b/s/Hz including the hard-decision forward error correction (HD-FEC) overhead). The variation of the optimum carrier-to-signal power ratio (CSPR) for different optical signal-to-noise ratio (OSNR) values was also investigated in simulations and experimentally verified. The accumulated dispersion along the fiber link was compensated using the electronic predistortion (EPD) technique, pre-compensation of the chromatic dispersion using transmitter-based DSP. The single channel and WDM signals were successfully transmitted over uncompensated standard single-mode fiber (SSMF) up to 727 and 323 km below the bit-error ratio (BER) of 3.8×10^{-3}, respectively.

II. Review of the WDM DD Experiments (ISD of $\geq$0.4 b/s/Hz)

Numerous experimental demonstrations of spectrally-efficient DD WDM systems have been reported to date, utilizing a variety of formats, including pulse amplitude modulation (PAM), (optical) duobinary ((O)DB), (e.g., phase-shaped binary transmission [7]), subcarrier modulation (SCM), namely Nyquist-subcarrier modulation (Nyquist-SCM) and orthogonal frequency division multiplexing (OFDM), and carrierless amplitude/phase modulation. The published experimental

Manuscript received February 13, 2015; revised April 3, 2015; accepted April 13, 2015. Date of publication April 27, 2015; date of current version June 20, 2015. This work was supported by the EU ERA-NET+ Project PIANO+ IMPACT, EPSRC UNLOC EP/J017582/1, and FP7 project ASTRON.

M. S. Erkılınç, Z. Li, B. C. Thomsen, P. Bayvel, and R. I. Killey are with the Optical Networks Group, Department of Electronic and Electrical Engineering, University College London, London WC1E 7JE, U.K. (e-mail: m.erkilinc@ee.ucl.ac.uk; zhe.li@ee.ucl.ac.uk; b.thomsen@ucl.ac.uk; p.bayvel@ucl.ac.uk; r.killey@ucl.ac.uk).

S. Pachnicke is with ADVA Optical Networking SE, 98617 Meiningen, Germany (e-mail: spachnicke@advaoptical.com).

H. Griesser is with ADVA Optical Networking SE, 82152 Martinsried, Germany (e-mail: hgriesser@advaoptical.com).

Color versions of one or more of the figures in this paper are available online at http://ieeexplore.ieee.org.

Digital Object Identifier 10.1109/JLT.2015.2427111

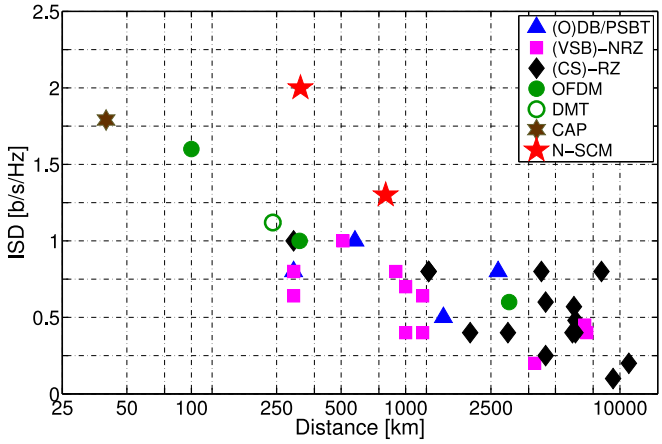

Fig. 1. Reported experimental demonstrations of WDM single polarization DD systems in terms of achieved net optical ISD versus distance. Formats: (VSB)-NRZ [8]–[15], (CS)-RZ[17]–[20], (O)DB [22]–[25], OFDM [29], [30], DMT [31] and Nyquist(N)-SCM [43] and this paper.

measurements of WDM single polarization transmission performance for the different modulation formats are summarised in Fig. 1 in which the net ISD versus maximum distance is plotted.

On-off keying (OOK), also referred to as 2-PAM, is the simplest modulation format to generate and detect. Several non-return-to-zero (NRZ) OOK experiments at an ISD of $<$0.5 b/s/Hz without the use of optical filtering at the transmitter have been demonstrated for submarine links [8], [9], as shown in Fig. 1. The ISD can be increased to 1 b/s/Hz with optical sideband or narrow filtering. Vestigial sideband (VSB) OOK experiments have been reported with ISDs of from 0.64 to 1 b/s/Hz [10]–[15]. Moreover, return-to-zero (RZ) OOK pulses with duty cycles of 33%, 50%, and 67% (carrier-suppressed RZ (CS-RZ)) can be generated using a pulse carver, typically a Mach–Zehnder modulator driven sinusoidally [16]. Among the binary signaling formats, CS-RZ has the highest resilience to fiber nonlinearity. It has been successfully demonstrated with ISDs of between 0.4 and 0.8 b/s/Hz for submarine and transoceanic links [17]–[19] and 1 b/s/Hz for metro distances [20]. Moreover, duobinary signaling, implemented using either optical or electrical filtering after differential pre-coding [21], has been proposed for both long- [22] and medium-haul optical communication systems with ISDs of up to 1 b/s/Hz [23]–[25].

The ISD of all the aforementioned modulation techniques is limited to 1 b/s/Hz due to their binary coding. Nyquist pulse-shaped four-level PAM (Nyquist 4-PAM) is a simple and low complexity multi-level format that potentially offers an ISD greater than 1 b/s/Hz. However, it suffers from low receiver sensitivity as it uses only one degree-of-freedom. Yet, it is attractive for very short distances, e.g., interconnects and intra-datacenter networks [26]. Alternatively, DSP-based transceiver architectures, enabled by high-speed digital-to-analog and analog-to-digital converters (DACs/ADCs), offering ISDs greater than 1 b/s/Hz using QAM signaling have started to be investigated since they offer higher receiver sensitivity than 4-PAM. In such transceiver architectures, SCM (e.g., Nyquist-SCM and OFDM) can be used for QAM signaling since the amplitude and phase of each subcarrier, also referred to as RF-subcarrier(s), can be recovered after photodetection from the optical carrier-signal beating products.

Direct detection optical OFDM (DDO-OFDM) has attracted much research interest for access, metro and regional applications. It uses multiple orthogonal subcarriers for encoding the data stream [27] (in contrast to Nyquist-SCM which uses a single subcarrier). DDO-OFDM offers a promising solution for metro and access applications due to its resilience to chromatic dispersion [27], and the possibility to use adaptive modulation on each subcarrier to handle the frequency response of a non-ideal link [28]. Recently, WDM DDO-OFDM experiments have been demonstrated with ISDs of 0.6 b/s/Hz over 3040 km [29], and 1.6 b/s/Hz over 100 km [30], as shown in Fig. 1. A real-valued OFDM signal, so-called discrete multi-tone (DMT), has also been demonstrated over 240 km of SSMF utilizing VSB signaling with an ISD of 1.12 b/s/Hz [31].

One disadvantage of SCM formats, such as DDO-OFDM and single SCM, is that they suffer from signal-signal beating interference (SSBI). Although a spectral guard-band can be used between the optical carrier and sideband, this reduces the ISD. Although some proposed optical or DSP-based methods to mitigate/cancel the SSBI, allowing the width of the guard-band to be reduced, have been shown to be effective, they come at the price of either a significant degradation in OSNR performance [32], increased optical complexity [33], digital complexity [34] or overheads [35]. High peak-to-average power ratio (PAPR) due to the constructive interference of the subcarriers, leading to high peaks in signal waveform, is another drawback for OFDM signals. This leads to the requirement for using high optical carrier power, to maintain unipolar modulation, and consequently, high required OSNR. It also necessitates an increase in the required dynamic range of the DACs/ADCs. Clipping is a practical low complexity solution to reduce the PAPR of the OFDM driving signals [36]. However, it comes at the expense of nonlinear distortion and penalties [27], [37], [38].

As an alternative to DDO-OFDM, the QAM symbols can be transmitted using a single subcarrier, a technique termed single SCM, to avoid the issue of high PAPR. To obtain the highest possible ISD, Nyquist pulse shaping with sideband filtering can be used. It has been shown that Nyquist pulse-shaped SCM signal formats have lower PAPR compared to DDO-OFDM and higher tolerance to SSBI [39]. For this reason, we have investigated the Nyquist-SCM modulation technique to extend the transmission distances and ISDs of DD WDM systems. The next section describes the Nyquist pulse-shaped SCM transceiver architecture and the simulation model.

III. Nyquist Pulse-Shaped SCM System Description and Transceiver DSP Design

In this section, first, the numerical simulations, that are carried out to optimize the Nyquist pulse-shaped SCM system characteristics to achieve a trade-off between the ISD and the required OSNR, are described. Then, the transceiver DSP design used in the simulations and experiments for offline signal generation and detection are outlined. The DD system architecture considered in this paper is shown in Fig. 2. The DD SCM technique utilizes linear optical field modulation to quadrature amplitude

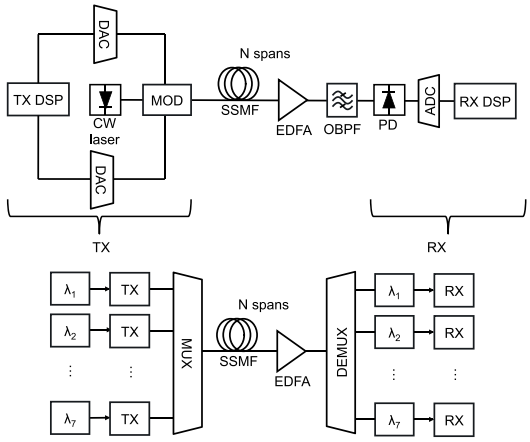

Fig. 2. System architecture for the single channel (top) and WDM system (bottom).

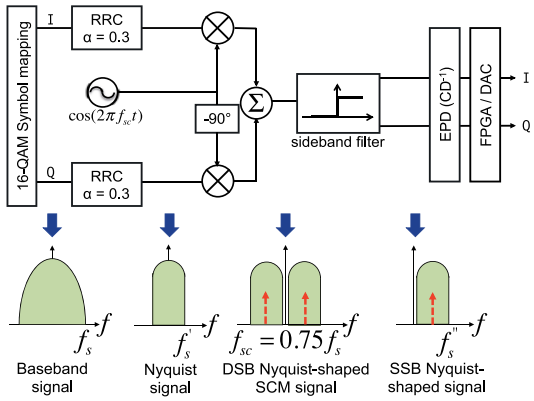

Fig. 3. Block diagram of Nyquist-SCM Transmitter DSP (top) and the schematic of the signal spectra of DSB and SSB three quarter-cycle ($f_{\rm sc} = 0.75 \times f_s$) Nyquist pulse-shaped ($\alpha = 0.3$) SCM (bottom). f_s: symbol rate, $f_{\rm sc}$: subcarrier frequency, $f_s^{'} = f_s/2(1+\alpha)$, $f_s^{''} = f_{\rm sc} + f_s^{'}$, EPD: Electronic pre-distortion and CD: Chromatic dispersion.

modulate a single subcarrier with M levels (M-QAM) [40]. After transmission over a fiber link, an optical band-pass filter (OBPF) is used to demultiplex the channel of interest. Detection is performed using a single-ended photodiode. Finally, the detected signal is sampled and quantized using a single ADC.

The optical ISD is determined by the frequency spacing ($f_{\rm sc}$) between the optical carrier and the subcarrier, and the choice of double sideband (DSB) or SSB signaling, the latter offering the lowest possible channel spacing. For the case of the DSB SCM format with $f_{\rm sc}$ equal to the symbol rate (f_s), the maximum ISD approaches $\log_2(M)/4$, referred to as single-cycle SCM [40]. The ISD can be increased towards $\log_2(M)/2$ through the use of Nyquist pulse shaping, and a reduction in the subcarrier frequency from f_s to f_s/2, referred to as half-cycle Nyquist-SCM [41]. A description of Nyquist pulse shaping in optical communication systems can be found in [42]. Combining this approach with SSB signaling results in ISDs approaching $\log_2(M)$. The half-cycle Nyquist-SCM with a roll-off factor (α) of 0 was first experimentally demonstrated for single channel case in [41]. Although using Nyquist pulse shaping filters with such a low roll-off factor maximises the ISD, it comes at the expense of lower tolerance to SSBI and high PAPR with the corresponding drawbacks, as briefly described in the previous section and discussed extensively in [39]. Therefore, a non-zero value for α can be used to achieve a trade-off between the spectral efficiency and the required OSNR. For the experiments and simulations described below, the values of α and $f_{\rm sc}$ were set to 0.3 and $0.75\times f_s$, respectively, since they provide a good compromise point as investigated in [43]. The SSB Nyquist-SCM transmitter DSP design is shown in Fig. 3. We have previously demonstrated single channnel and WDM systems utilizing SSB Nyquist pulse-shaped QPSK SCM in back-to-back operation [44] and transmission over 800 km of SSMF [43] with a net optical ISD of 1.2 b/s/Hz, plotted in Fig. 1.

Transmission simulations were carried out with MATLAB using the split-step Fourier method to solve the nonlinear Schrödinger equation. Four 2^{18} patterns, based on a de Bruijn binary sequence and decorrelated by 0.25 of the pattern length, were mapped to 16-QAM symbols. A pair of root raised-cosine (RRC) pulse-shaping filters with $\alpha = 0.3$, 256 taps and a stop-band attenuation of 40 dB were applied to the in-phase (I) and quadrature (Q) components to generate the digital representation of the Nyquist pulse-shaped signal. The I- and Q-components were up-converted to a subcarrier frequency ($f_{\rm sc}$) of 4.68 GHz ($0.75\times f_s$) and added to each other to obtain a DSB Nyquist pulse-shaped SCM signal at a bit rate of 25 Gb/s, as shown in Fig. 3. DSB to SSB conversion was performed using a digital sideband filter, followed by EPD, implemented in the frequency domain to mitigate the chromatic dispersion at the targeted distances. As described in [45] and [46], the spectrum of the pre-dispersed signal, $E(\omega,0)$ can be written as:

$$\begin{aligned} E(\omega,0) &= E(\omega,L)H^{-1}(\omega) \\ &= E(\omega,L)\exp\left(j\frac{D}{4\pi c}\lambda^2\omega^2 L\right) \end{aligned} \tag{1}$$

where $E(\omega,L)$ is the desired optical field of the signal at the end of the link of length L, $H^{-1}(\omega)$ is the inverse of the transfer function of the fiber (neglecting loss and nonlinearity), λ is the wavelength, c is the speed of light in vacuum, D is the fiber dispersion and ω is the angular frequency. Finally, the real and imaginary parts of the pre-dispersed signal (Re$\{F^{-1}[E(\omega,0)]\}$ and Im$\{F^{-1}[E(\omega,0)]\}$) were quantized to 6 bits (the nominal resolution of the DACs (Micram VEGA DACII) used in the experiments) and uploaded to the FPGA-RAM memory blocks. To demonstrate the fundamental limits of the proposed transceiver, simulations were performed assuming near ideal conditions, considering an effective number of bits (ENOB) of 6 bits and a sampling rate of 28 GSa/s while neglecting bandwidth limitations. Then, the practical parameters were taken into account, i.e., setting the electrical signal-to-noise (SNR) to 23 dB to take into account the ENOB of the practical DACs (3.8 bits at 10 GHz) and, applying electrical fifth-order Bessel low-pass filters (LPFs) at the transmitter and receiver sides with bandwidths of 7 and 16 GHz, respectively, to emulate the frequency response of the anti-imaging/-aliasing filters. To model the WDM transmission, 7×12 GHz-spaced channels carrying 25 Gb/s SSB Nyquist pulse-shaped 16-QAM SCM signals were generated and decorrelated by 490 samples.

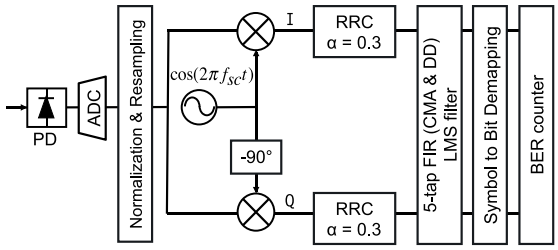

Fig. 4. Block diagram of Nyquist-SCM Receiver DSP. CMA: Constant modulus algorithm, DD: Decision-directed, LMS: Least mean squares and FIR: Finite-impulse response.

The transmission link considered in the simulations consisted of uncompensated SSMF and EDFAs with a noise figure of 5 dB. The fiber parameters α, D, γ and $L_{\rm span}$ were chosen as 0.2 dB/km, 17 ps/(nm·km), 1.2 $\rm W^{-1}{\cdot}km^{-1}$ and 80 km, respectively. An additional loss of 15 dB per amplifier span was included to take into account the effects of additional optical components. All amplified spontaneous emission (ASE)-noise generated by the EDFAs was added inline to model nonlinear signal-ASE noise interaction. The symmetric split-step Fourier method [47] was utilized to model the single channel and WDM transmission at a simulation bandwidth of 200 GHz with step sizes of 1 km and 400 m, respectively.

To demultiplex the channel of interest and remove the out-of-band ASE-noise before the photodiode, first an ideal brickwall-shaped OBPF for ideal system simulations and subsequently, a fourth-order super-Gaussian OBPF for the practical system simulations were applied. The transmitted optical signal was detected by a single-ended photodiode with a responsivity of 1 A/W, followed by an ADC with a resolution of 5-bits and a sampling rate of 50 GSa/s, and finally the receiver DSP, a block diagram of which is shown in Fig. 4. After the digitized received signal was normalized and resampled to 2 samples/symbol, the signal was split into two branches and down-converted to generate baseband I- and Q-components. Then, a pair of matched RRC filters with $\alpha = 0.3$ were applied to the components, separately. Before the symbol-to-bit demapping, 5-tap FIR filtering was performed for symbol re-timing. The cost function was chosen as the constant modulus algorithm to update the filter taps for fast convergence, before switching to decision directed least-mean squares (LMS). Finally, the BER was calculated over 2^{20} bits by error counting. The transmission results are presented in terms of Q^2-factor ($Q^2[\rm dB] = 20\log_{10}(\sqrt{2}\rm erfcinv(2\mathit{p_b}))$ where p_b is the BER. To calculate the net bit rate and net ISD, the hard decision decoding bound for the binary symmetric channel was utilized such that the maximum code rate (r) is given by [48]

$$r = 1 + p_b \log_2 p_b + (1 - p_b)\log_2(1 - p_b). \tag{2}$$

At a BER of 3.8×10^{-3}, r was found to be 0.96. Hence, the net bit rate per channel was 24 Gb/s (25 Gb/s$\times r$), resulting in a net optical ISD of 2.0 b/s/Hz (2.08 b/s/Hz$\times r$) for the WDM transmission. The simulation results for back-to-back and transmission cases are discussed together with the experimental results in Section V.

IV. Transmission Experiments

The optical transmission test-bed consisted of a 7×25 Gb/s channel SSB Nyquist pulse-shaped 16-QAM SCM transmitter, an optical fiber recirculating loop and a DD receiver to detect the channel of interest, as shown in Fig. 5. An external cavity laser (ECL) with a linewidth of 100 kHz at 1550 nm was used as the seed for an optical comb generator (OCG) based on cascaded amplitude and phase modulators to generate seven 12 GHz-spaced unmodulated optical channels, as shown in Fig. 5. Although a laser source with higher linewidth could be used in DD SCM, an ECL was used due to its availability. The number of comb lines was limited to seven in order to maintain the power variation across the channels to within 1 dB. The channel spacing was chosen to ensure the penalty caused by linear crosstalk due to the neighboring channels was $\leq$1 dB. Odd ($\lambda_{1,3,5,7}$) and even ($\lambda_{2,4,6}$) channels were separated using three cascaded Kylia micro-interferometer interleavers with a suppression of 40 dB to allow independent modulation with uncorrelated bit sequences.

As shown in Fig. 3(a), the signal waveforms used for driving the IQ-modulators were generated offline in MATLAB using four 2^{15} de Bruijn bit sequences, de-correlated by 0.25 of the pattern length. The waveforms were uploaded to the memory of a pair of Xilinx Virtex-5 FPGAs to drive the DACs. To prevent crosstalk between WDM channels due to the images generated by the DACs, electrical anti-imaging filters, fifth-order Bessel LPFs with a bandwidth of 7 GHz, were used. An optical SSB signal with an OSNR of 34 dB at a resolution of 0.1 nm was generated using the IQ-modulators with a switching voltage (V_π) of 3.5 V. The modulators were driven by the electrical signals with a peak-to-peak voltage (V_{pp}) of 3.4 V. Note that the IQ-modulators were biased close to their quadrature points to achieve approximately linear mapping from the electrical to the optical domain with the bias voltages adjusted to achieve the desired optical carrier power. In DD links, the optimum optical carrier power value is dependent on the sideband power and is specified as the CSPR:

$$\text{CSPR(dB)} = 10\log_{10}\left(\frac{P_C}{P_S}\right), \tag{3}$$

where P_C and P_S are the optical carrier and sideband powers, respectively. The CSPR is discussed in more detail in Section V-A. Decorrelating fiber of 1 km length (delay of 17 ns corresponding to approximately 425 samples) was used to decorrelate the odd and even channels before they were combined and launched into the recirculating loop. The optical spectra of modulated odd and even channels are shown together in Fig. 5(b). Note that the optical spectra shown in Fig. 5(a)–(c) are taken from the optical spectrum analyser (OSA) at a resolution of 0.01 nm.

The transmission experiment was performed using an optical recirculating loop with a single span of 80.7 km ($D_{\rm SSMF}$ =17 ps/nm/km), as shown in Fig 5. The loop was controlled by two switches (AOM Tx and AOM Loop) to switch from "signal TX" to "signal loop" stage. An OBPF (Yenista Optics XTM50-Wide) with a 3 dB bandwidth of 200 GHz and a filter edge gradient of 500 dB/nm was used to filter the

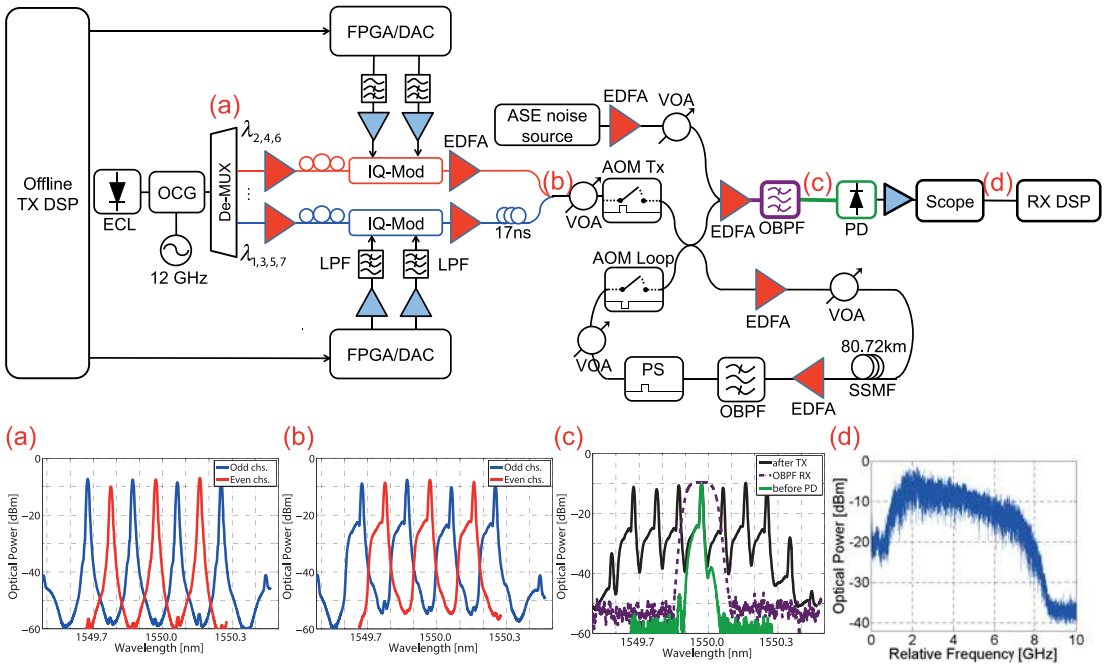

Fig. 5. Experimental setup for WDM SSB Nyquist pulse-shaped SCM transmission. Note that the block diagram of offline TX and RX DSP are presented in Fig. 3 and Fig. 4, respectively. FPGA: Field programmable gate array, VOA: Variable optical attenuator, AOM: Acousto-optic modulator, PS: Polarization scrambler, PD: Photodiode. Insets: Experimental optical spectra of 7 channels (a) after OCG, (b) after the transmitter and (c) transmitted optical signal, OBPF response at the receiver and received optical signal. (d) Received electrical spectrum.

out-of-band ASE-noise during the transmission. A loop synchronous polarization scrambler was utilized to randomize the signal polarization state in each span. The launch power into the span was controlled by the variable optical attenuators (VOAs). The fiber loss of 16 dB plus the combined loss of 15 dB from the VOAs, PS, AOM and OBPF resulted in a total loss per recirculation of 31 dB, which was compensated by two EDFAs with a noise figure of 5 dB, operating at their saturation point (18 dBm output power).

At the receiver, the channel of interest was demultiplexed using a tunable OBPF (Yenista Optics XTM50-Ultrafine) with a 3 dB bandwidth of 11 GHz and a filter edge gradient of 800 dB/nm, as shown in Fig. 5(c). The filter was tuned manually to optimize the system performance. The demultiplexed optical signal was detected by a single-ended photodiode, followed by an RF-amplifier to boost the signal power. The amplified electrical signal was acquired using a single ADC (Tektronix DPO 72004 oscilloscope) operating at 50 GSa/s with an electrical bandwidth of 16 GHz and a nominal resolution of 8 bits (ENOB of 5 bits at 10 GHz). The digitized signal spectrum is shown in Fig. 5(d). The signal was decoded for BER counting, as described in Section III with the block diagram illustrated in Fig. 4. The BER was calculated over 2^{20} bits by error counting and the Q^2-factor was computed from the measured BER.

V. Transmission Results and Discussions

The BER and Q^2-factor measurements were carried out for single channel and WDM systems operating at a bit rate of 25 Gb/s. The signal quality was assessed first in back-to-back, and then after transmission over a variety of distances.

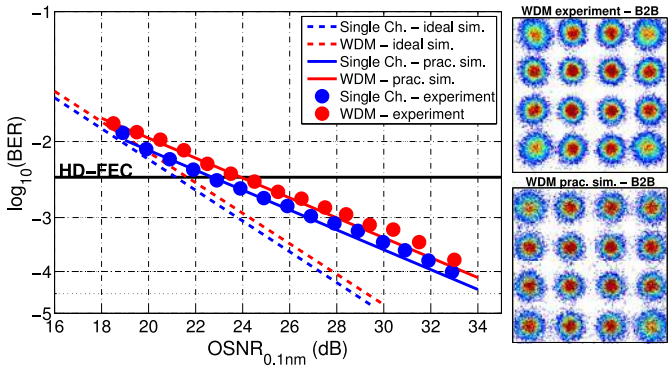

Fig. 6. Simulated and experimental BER versus OSNR curves for back-to-back case (left). Experimental and simulated WDM signal constellations at an OSNR of 34 dB (right).

ASE-noise loading to characterize back-to-back operation was performed at the receiver. To optimize the system performance, CSPR values were varied at different OSNR values. For WDM transmission, the BER was measured for all seven transmitted channels.

A. Back-to-Back Performance

Simulated and experimentally measured back-to-back BERs with respect to OSNR for single channel and WDM systems are presented in Fig. 6. Ideal system simulations, neglecting practical limitations such as DACs/ADC quantization noise and optical/electrical filtering effect, indicated that the required OSNR at the HD-FEC threshold in single channel back-to-back operation is 21 dB for the SSB Nyquist pulse-shaped 16-QAM

SCM signal with $\alpha = 0.3$ and $f_{sc} = 4.68$ GHz ($0.75 \times f_s$). In our experiments, the required OSNR for single channel was measured to be 23 dB, a 2 dB implementation penalty with respect to the ideal simulation results. This was accounted for by the DACs/ADC quantization noise, low-pass filtering and non-ideal optical filtering at the receiver. Moreover, for the WDM system, an additional 1 dB penalty was observed due to the linear crosstalk caused by the neighboring channels. This additional penalty was not observed in ideal system simulations because a brickwall-shaped OBPF was used to demultiplex the channel of interest. The implementation penalties both in single channel and WDM systems were verified by simulations using practical parameters, as shown with blue and red solid lines in Fig. 6. To take into account the non-idealities of our experiment, the SNR of the electrical driving signals was set to 23 dB, emulating the DACs' ENOB, and ADC resolution was set to 5 bits. In addition to quantization noise, a fourth-order super-Gaussian-shaped OBPF with a bandwidth of 11 GHz was used to filter out the out-of-band ASE-noise and demultiplex the central WDM channel. There is good agreement between experimental and simulated BER values and constellations for single channel and WDM systems, as can be seen in Fig. 6.

In SCM-based DD systems, it is crucial to optimize the CSPR to achieve the minimum BER at a given OSNR. Thus, we investigated the system sensitivity to CSPR variation, both in simulations and experimentally. To measure the CSPR value at a given OSNR accurately, two different methods were assessed. First, the transmitted signal was split into two arms and, one arm was detected using a coherent receiver whilst the other arm was detected by the DD receiver for BER counting, as explained in Section IV. After the optical full-field was recovered using the coherent receiver, two brickwall-shaped digital filters were used to filter out the optical carrier and sideband. The corresponding power values for the carrier and sideband were computed and the resulting CSPR value was determined using Eq. (3). Since the measurement was carried out at a very high resolution (approximately 100 kHz), it is the most accurate method to measure the CSPR. In a simpler alternative approach, we measured the CSPR at a given OSNR using the corresponding optical spectrum taken from the OSA at a resolution of 0.01 nm. After the spectrum was acquired, the carrier and sideband power were measured using two fifth-order super-Gaussian-shaped filters in MATLAB, similar to the first method. Finally, the measured CSPR values using the two different methods were compared and a discrepancy of approximately 10% was found. Since the second, simpler method was sufficiently accurate for our demonstrations, the majority of the CSPR values were measured using the second method.

The BER as a function of CSPR for six different OSNR values is shown in Fig. 7. The CSPR value was varied between 4 and 16 dB for OSNR values ranging from 19 to 29 dB. The dashed red arrow indicates how the optimum CSPR shifts towards higher values as the OSNR is increased. At low CSPR values, the system is SSBI-limited since the signal-signal mixing products distort the desired signal (carrier-signal mixing products) severely. On the other hand, in the high CSPR regime, signal-ASE beating noise limits the system performance. The simulation results shown with the solid lines closely match the

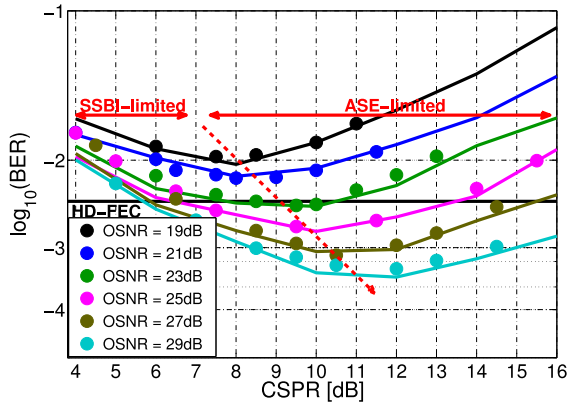

Fig. 7. Simulated and experimental BER with respect to CSPR at different OSNR levels in back-to-back operation. The dashed red arrow indicates the shift in the optimum CSPR value.

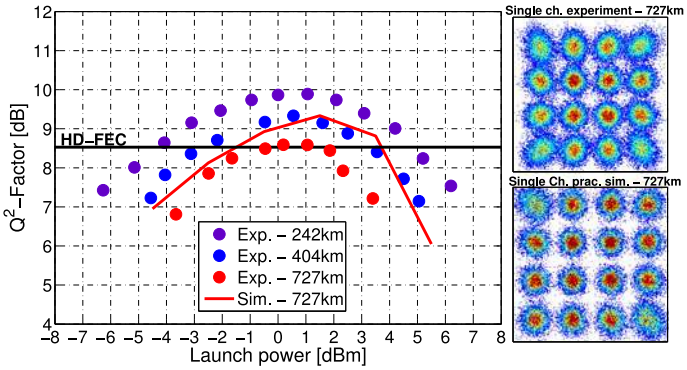

Fig. 8. Q^2-factor versus launch power per channel for single channel (left) and corresponding experimental and simulated constellations at a distance of 727 km and at the optimum launch power of 1 dBm.

experimental results shown with the markers in Fig. 7. It was found that optimum CSPR values were similar for single channel and WDM systems in back-to-back operation.

B. Transmission Performance

After back-to-back characterization, single channel and WDM transmission experiments were performed. Single channel transmission was carried out for distances from 242 km up to 727 km (up to nine spans) using the recirculating fiber loop. The experimental Q^2-factor values for single channel transmission distances of up to 727 km and the simulated Q^2-factor values for 727 km transmission with respect to the launch power per channel are shown in Fig. 8. It was found that the simulated and experimental results are similar which can also be observed in the constellations shown in Fig. 8. In single channel transmission, the optimum launch power was found to be approximately 1 dBm. BER values below the FEC threshold were obtained for launch powers over the range from -4 to 4 dBm at 242 km. This range decreased when the transmission distance increased as expected. The maximum achieved transmission distance was 727 km at a launch power of 1 dBm with the measured BER/Q^2-factor of 3.5×10^{-3}/8.7 dB, just achieving the HD-FEC threshold. The optimum CSPR value was found to be approximately 8 dB at 727 km in single channel transmission.

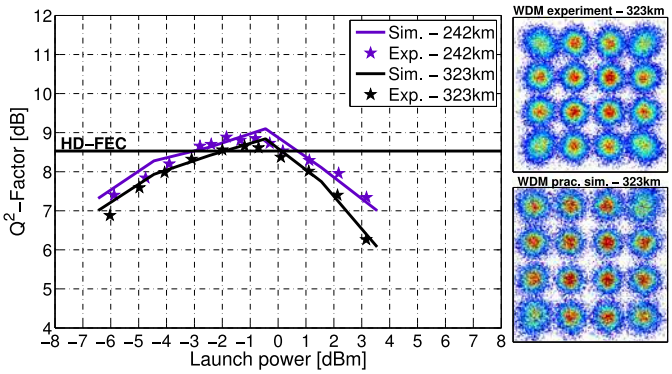

Fig. 9. Q^2-factor versus launch power per channel for WDM system (left) and corresponding experimental and simulated constellations at a distance of 323 km and at the optimum launch power of −1.6 dBm.

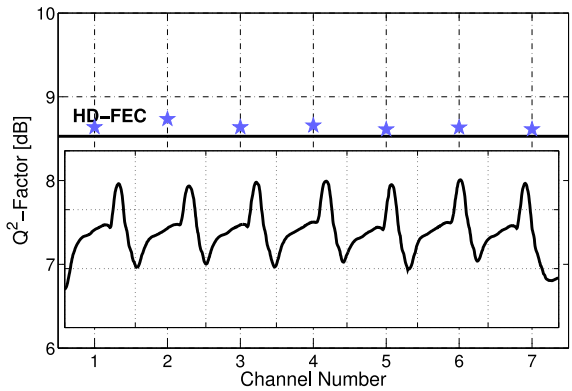

Fig. 10. Q^2-factor for each received channel at 323 km. Inset: Transmitted optical spectrum.

The seven-channel WDM transmission distances of 242 and 323 km were achieved with maximum Q^2-factors of 9 and 8.7 dB, respectively, at a launch power of −1.6 dBm per channel, as shown in Fig. 9 with their corresponding constellations. In the linear regime, WDM achieves the same Q^2-factor value at a slightly higher launch power per channel compared to the single channel transmission. This is due to the linear crosstalk caused by the neighbouring channels which was also observed in the back-to-back operation (see Fig. 6). Due to the additional inter-channel nonlinear effects during WDM transmission compared to single channel transmission, the maximum transmission distance was reduced from 727 to 323 km. There is very good agreement between the transmission experiments and simulations. The optimum CSPR value was found to be approximately 7 dB in WDM transmission at 323 km, slightly lower than the single channel transmission at 727 km. This small change in the optimum CSPR value is due to the trade-off between the SSBI and fiber nonlinearities, and, as expected, the optimum CSPR value is lower in WDM transmission because of the fiber nonlinearities.

All seven channels operating at 25 Gb/s achieved a BER$<3.8\times10^{-3}$ (Q^2-factor>8.52 dB) at the optimum launch power of −1.6 dBm per channel, as shown in Fig. 10. Hence, a total net bit rate of 168 Gb/s (7ch.×25 Gb/s×r) with a net ISD of 2.0 b/s/Hz was achieved over 323 km of SSMF. This is plotted in Fig. 1 and, relative to the previous experiments, it is at the highest ISD reported for DD systems at this transmission distance.

It is of interest to compare the complexity of the optical hardware of the Nyquist-SCM system with that of an equivalent coherent polarization division multiplexed (PDM) 16-QAM targeting the same bit rate. Assuming the same electrical bandwidth for both systems, and with the transmitter DSP approach described in this paper, four WDM channels are required to reach the same data rate as opposed to a single PDM 16-QAM channel (e.g., 4×28 Gb/s at 7 GBaud with 16-QAM Nyquist-SCM using DD versus 1×112 Gb/s at 14 GBaud with coherent PDM 16-QAM). However, the SSB Nyquist-SCM scheme can be also realized shifting the optical carrier frequency by the IQ-modulators during modulation, enabling the full bandwidth of the IQ-modulators to be used as described in [34] and [49]. Consequently, this configuration would allow a symbol rate of 14 GBaud using a single IQ-modulator, and hence, the required number of channels can be halved (e.g., 2× 56 Gb/s at 14 GBaud). In this case, the DD Nyquist-SCM system would require two transmitter lasers, two IQ-modulators and two photodiodes. In contrast, the coherent PDM 16-QAM system requires a single transmitter laser and a local oscillator laser, two IQ-modulators, and eight photodiodes (four balanced detectors), in addition to polarization beam splitting/combining optics and a pair of optical hybrids. The simplified optical structure of the Nyquist-SCM scheme comes at the expense of lower maximum transmission distance and information spectral density since only a single polarization is used and optical filtering, rather than digital filtering, determines the achievable channel spacing.

VI. Summary and Conclusion

We experimentally demonstrated, for the first time, single channel and WDM Nyquist pulse-shaped 16-QAM SCM with a net optical information spectral density of 2.0 bits/s/Hz using a simple DD receiver (a single-ended photodiode and a single ADC). Back-to-back and transmission performance was assessed for ideal and practical configurations. First, simulations of the ideal system (with minimal DACs/ADC quantization noise and neglecting electrical bandwidth limitations) for the back-to-back case were performed to investigate the fundamental limits of the proposed system and to quantify the implementation penalties of the practical system (2 dB for single channel and 3 dB for WDM). Then, the experimental results on single channel and seven-channel WDM system performance for back-to-back and transmission cases were verified by simulations of the practical system. The effect of varying the CSPR at different OSNR values was also simulated and experimentally measured for the back-to-back case.

The maximum achievable transmission distance over EDFA-only amplified SSMF with 31 dB loss per span (the fiber loss plus the total insertion loss due to the loop components) was 727 km for the single channel case, whereas the transmission distance decreased to 323 km in WDM case mainly due to inter-channel nonlinear effects. The EPD technique, pre-dispersing the signal at the transmitter DSP, was utilized to mitigate the chromatic dispersion accumulated along the fiber. To the best of our knowledge, this is the highest achieved ISD, at this distance,

among the reported experimental WDM demonstrations in DD links using a single-ended photodiode and a single ADC. The results indicate that DD Nyquist pulse-shaped SCM can be an attractive approach offering high information spectral density and cost-effective transceiver design, and thus, may be practical for metro, regional and access applications.

REFERENCES

[1] Alcatel-Lucent, "Bell Labs metro network traffic growth: An architecture impact study," Strategic White Paper, Dec. 2013.

[2] *Cisco Visual Networking Index: Forecast and Methodology, 2013–2018*, Cisco, San Jose, CA, USA, 2014.

[3] S. Savory, "Digital filters for coherent optical receivers," *Opt. Exp.*, vol. 16, no. 2, pp. 804–817, 2008.

[4] M. Mazurczyk, "Spectral shaping in long haul optical coherent systems with high spectral efficiency," *J. Lightw. Technol.*, vol. 32, no. 16, pp. 2915–2924, Aug. 2014.

[5] J. X. Cai, "100G transmission over transoceanic distance with high spectral efficiency and large capacity," *J. Lightw. Technol.*, vol. 30, no. 24, pp. 3845–3856, Dec. 2012.

[6] ADVA. (2014). Efficient 100G transport. [Online]. Available: http://www.advaoptical.com/en/innovation/100g-transport.aspx

[7] D. Penninckx, M. Chbat, L. Pierre, and J. P. Thiery, "The phase-shaped binary transmission (PSBT): A new technique to transmit far beyond the chromatic dispersion limit," *IEEE Photon. Technol. Lett.*, vol. 9, no. 2, pp. 259–261, Feb. 1997.

[8] C. R. Davidson, C. J. Chen, M. Nissov, A. Pilipetskii, N. Ramanujam, H. D. Kidorf, B. Pedersen, M. A. Mills, C. Lin, M. I. Hayee, J. X. Cai, A. B. Puc, P. C. Corbett, R. Menges, H. Li, A. Elyamani, C. Rivers, and N. S. Bergano, "1800 Gb/s transmission of one hundred and eighty 10 Gb/s QDM channels over 7000 km using the full EDFA C-band," presented at the Opt. Fiber Commun. Conf., Baltimore, MD, USA, 2000, Paper PD25.

[9] G. Vareille, F. Pitel, and J. F. Marcerou, "3 Tbit/s (300 × 11.6 Gbit/s) transmission over 7380 km using C+ L band with 25GHz channel spacing and NRZ format," presented at the Opt. Fiber Commun. Conf., Amsterdam, The Netherlands, 2001, Paper PD22.

[10] S. Bigo, W. Idler, J.-C. Antona, G. Charlet, C. Simonneau, M. Gorleir, M. Molina, S. Borne, C. de Barros, P. Sillard, P. Tran, R. Dischler, W. Poehlmann, P. Nouchi, and Y. Frignac, "Transmission of 125 WDM channels at 42.7 Gbit/s (5 Tbit/s capacity) over 12 × 100 km of TeraLight ultra fibre," presented at the Eur. Conf. Opt. Commun., Amsterdam, The Netherlands, 2001, Paper PD.M.1.1.

[11] W. Idler, S. Bigo, Y. Frignac, B. Franz, and G. Veith, "Vestigial side-band demultiplexing for ultra-high capacity (0.64 bit/s/Hz) of 128 × 40 Gbit/s channels," presented at the Opt. Fiber Commun. Conf., Anaheim, CA, USA, 2001, Paper MM3.

[12] S. Bigo, A. Bertaina, Y. Frignac, S. Borne, L. Lorcy, D. Hamoir, D. Bayart, J.-P. Hamaide, W. Idler, E. Lach, B. Franz, G. Veith, P. Sillard, L. Fleury, P. Guénot, and P. Nouchi, "5.12 Tbit/s (128 × 40 Gbit/s WDM) transmission over 3 × 100 km of TeraLight fiber," presented at the Eur. Conf. Opt. Commun., Munich, Germany, 2000, Paper PD1.2.

[13] W. Idler, G. Charlet, R. Dischler, Y. Frignac, and S. Bigo, "0.8 bit/s/Hz of information spectral density by vestigial side-band filtering of 42.66 Gb/s NRZ," presented at the Eur. Conf. Opt. Commun., Copenhagen, Denmark, 2002, Paper 8.1.5.

[14] G. Charlet, J.-C. Antona, P. Tran, S. Bigo, W. Idler, and R. Dischler, "3.2 Tbit/s (80 × 42.7 Gb/s) C-band transmission over 9 × 100 km of TeraLight fiber with 50 GHz channel spacing," presented at the Top. Meet. Opt. Amplifiers Appl., Vancouver, Canada, 2002, Paper PDP1.

[15] K. Schuh, E. Lach, B. Junginger, G. Veith, J. Renaudier, G. Charlet, and P. Tran, "8 Tbit/s (80 × 107 Gbit/s) DWDM ASK-NRZ VSB transmission over 510 km NZDSF with 1 bit/s/Hz spectral efficiency," presented at the Eur. Conf. Opt. Commun., Berlin, Germany, 2007, Paper PD1.8.

[16] E. Ip and J. M. Kahn, "Power spectra of return-to-zero optical signals," *J. Lightw. Technol.*, vol. 24, no. 3, pp. 1610–1618, Mar. 2006.

[17] J.-X. Cai, M. Nissov, C. R. Davidson, Y. Cai, A. N. Pilipetskii, H. Li, M. A. Mills, R. -M. Mu, U. Feiste, L. Xu, A. J. Lucero, D. G. Foursa, and N. S. Bergano, "Transmission of thirty-eight 40 Gb/s channels (>1.5 Tb/s) over transoceanic distance," presented at the Opt. Fiber Commun. Conf., Anaheim, CA, USA, 2002, Paper FC4.

[18] Y. Frignac, G. Charlet, W. Idler, R. Dischler, P. Tran, S. Lanne, S. Borne, C. Martinelli, G. Veith, A. Jourdan, J.-P. Hamaide, and S. Bigo, "Transmission of 256 wavelength-division and polarization-division multiplexed channels at 42.7 Gb/s (10.2 Tb/s capacity) over 3 × 100 km of TeraLight fiber," presented at the Opt. Fiber Commun. Conf., Anaheim, CA, USA, 2002, Paper FC5.

[19] D. F. Grosz, A. Agarwal, S. Banerjee, A. P. Kung, D. N. Maywar, A. Gurevich, T. H. Wood, C. R. Lima, B. Faer, J. Black, and C. Hwu, "5.12 Tb/s (128 × 42.7 Gb/s) transmission with 0.8 bit/s/Hz spectral efficiency over 1280 km of standard single-mode fiber using all-Raman amplification and strong signal filtering," presented at the Eur. Conf. Opt. Commun., Copenhagen, Denmark, 2002, Paper PD4.3.1.

[20] I. Morita, T. Tsuritani, N. Yoshikane, A. Agata, K. Imai, and N. Edagawa, "100% Spectral–efficient 25 × 42.7 Gbit/s transmission using asymmetric filtered CS-RZ signal and a novel crosstalk suppressor," presented at the Eur. Conf. Opt. Commun., Copenhagen, Denmark, 2002, Paper PD4.7.

[21] E. Pincemin, C. Gosset, N. Boudrioua, A. Tan, D. Grot, and T. Guillossou, "Experimental performance comparison of duobinary and PSBT modulation formats for long-haul 40 Gb/s transmission on G 0.652 fibre," *Opt. Exp.*, vol. 20, no. 27, pp. 28171–28190, 2012.

[22] G. Charlet, S. Lanne, L. Pierre, C. Simonneau, P. Tran, H. Mardoyan, P. Brindel, M. Gorlier, J.-C. Antona, M. Molina, P. Sillard, J. Godin, W. Idler, and S. Bigo, "Cost-optimized 6.3 Tbit/s-capacity terrestrial link over 17 × 100 km using phase-shaped binary transmission in a conventional all-EDFA SMF-based system, presented at the Opt. Fiber Commun. Conf., Atlanta, GA, USA, 2003, Paper PD2.5.

[23] T. Ono, Y. Yano, K. Fukuchi, T. Ito, H. Yamazaki, M. Yamaguchi, and K. Emura, "Characteristics of optical duobinary signals in terabit/s capacity, high-spectral efficiency WDM systems," *J. Lightw. Technol.*, vol. 16, no. 5, pp. 788–797, May 1998.

[24] H. Bissessur, G. Charlet, W. Idler, C. Simonneau, S. Borne, L. Pierre, R. Dischler, C. de Barros, and P. Tran, "3.2 Tbit/s (80 × 40 Gbit/s) phase-shaped binary transmission over 3 × 100 km with 0.8 bit/s/Hz efficiency," *Electron. Lett.*, vol. 38, no. 8, pp. 377–379, 2002.

[25] M. Alfiad and S. Tibuleac, "100G superchannel transmission using 4 × 28 Gb/s subcarriers on a 25-GHz Grid," *IEEE Photon. Technol. Lett.*, vol. 27, no. 2, pp. 157–160, Jan. 2015.

[26] J. L. Wei, J. D. Ingham, D. G. Cunningham, R. V. Penty, and I. H. White, "Performance and power dissipation comparisons between 28 Gb/s NRZ, PAM, CAP and optical OFDM systems for data communication applications," *J. Lightw. Technol.*, vol. 30, no. 20, pp. 3273–3280, Oct. 2012.

[27] A. J. Lowery and L. B. Du, "Optical orthogonal division multiplexing for long haul optical communications: A review of the first five years," *Opt. Fiber Technol.*, vol. 17, pp. 421–438, 2011.

[28] E. Giacoumidis, A. Kavatzikidis, A. Tsokanos, J. M. Tang, and I Tomkos, "Adaptive loading algorithms for IMDD optical OFDM PON systems using directly modulated lasers," *J. Opt. Commun. Network.*, vol. 4, no. 10, pp. 769–778, 2012.

[29] Z. Li, X. Xiao, T. Gui, Q. Yang, R. Hu, Z. He, M. Luo, C. Li, X. Zhang, D. Xue, S. You, and S. Yu, "432-Gb/s direct-detection optical OFDM superchannel transmission over 3040-km SSMF," *IEEE Photon. Technol. Lett.*, vol. 25, no. 15, pp. 1524–1526, Aug. 2013.

[30] H. Chen, M. Chen, F. Yin, M. Xin, and S. Xie, "100Gb/s PolMux-NRZ-AOS-OFDM transmission system," *Opt. Exp.*, vol. 17, no. 21, pp. 18768–18773, 2009.

[31] A. Dochhan, H. Grieser, M. Eiselt, J.-P. Elbers, "Flexible bandwidth 448 Gb/s DMT transmission for next generation data center inter-connects," presented at the Eur. Conf. Opt. Commun., Cannes, France, 2014,

[32] Y. Zhang, M. O'Sullivan, and R. Hui, "Theoretical and experimental investigation of compatible SSB modulation for single channel long-distance optical OFDM transmission," *Opt. Express*, vol. 18, no. 16, pp. 16751–16764, 2010.

[33] S. A. Nezamalhosseini, L.R. Chen, Q. Zhuge, M. Malekiha, F. Marvasti, and D. V. Plant, "Theoretical and experimental investigation of direct detection optical OFDM transmission using beat interference cancellation receiver," *Opt. Exp.*, vol. 21, no. 13, pp. 15237–15246, 2013.

[34] W.-R. Peng, B. Zhang, K.-M. Feng, X. Wu, A. E. Willner, and S. Chi, "Spectrally efficient direct-detected OFDM transmission incorporating a tunable frequency gap and an iterative detection techniques," *J. Lightw. Technol.*, vol. 27, no. 24, pp. 5723–5735, Dec. 2009.

[35] Z. Cao, J. Yu, W. Wang, L. Chen, and Z. Dong, "Direct-detection optical OFDM transmission system without frequency guard band," *IEEE Photon. Technol. Lett.*, vol. 22, no. 11, pp. 736–738, Jun. 2010.

[36] T. Jiang and Y. Wu, "An overview: Peak-to-average power ratio reduction techniques for OFDM signals," *IEEE Trans. Broadcast.*, vol. 54, no. 2, pp. 257–268, Jun. 2008.

[37] J. Armstrong, "OFDM for optical communications," *J. Lightw. Technol.*, vol. 27, no. 3, pp. 189–204, Feb. 2009.

[38] C. R. Berger, Y. Benlachtar, R. I. Killey, and P. A. Milder, "Theoretical and experimental evaluation of clipping and quantization noise for optical OFDM," *Opt. Exp.*, vol. 19, no. 18, pp. 17713–17728, 2011.

[39] M. S. Erkılınç *et al.*, "Performance comparison of single sideband direct detection Nyquist-subcarrier modulation and OFDM," *J. Lightw. Technol.*, vol. 33, no. 10, pp. 2038–2046, May 2015.
[40] A. O. J. Wiberg, B. Olsson, and P. A. Andrekson, "Single cycle subcarrier modulation," presented at the Opt. Fiber Commun. Conf., San Diego, CA, USA, 2009, Paper OTuE.1.
[41] A. S. Karar and J. C. Cartledge, "Generation and detection of a 112-Gb/s dual polarization signal using a directly modulated laser and half-cycle 16-QAM Nyquist-subcarrier-modulation," presented at the Eur. Conf. Opt. Commun., Amsterdam, The Netherlands, 2012, Paper Th3.A.4.
[42] G. Bosco, A. Carena, V. Curri, P. Poggiolini, and F. Forghieri, "Performance limits of Nyquist-WDM and CO-OFDM in high-speed PM-QPSK systems," *IEEE Photon. Technol. Lett.*, vol. 22, no. 15, pp. 1129–1131, Aug. 2010.
[43] M. S. Erkılınç, S. Kilmurray, R. Maher, M. Paskov, R. Bouziane, S. Pachnicke, H. Griesser, B. C. Thomsen, P. Bayvel, and R. I. Killey, "Nyquist-shaped dispersion-precompensated subcarrier modulation with direct detection for spectrally-efficient WDM transmission," *Opt. Exp.*, vol. 22, no. 8, pp. 9420–9431, 2014.
[44] M. S. Erkilinc, R. Maher, M. Paskov, S. Kilmurray, S. Pachnicke, H. Griesser, B. C. Thomsen, P. Bayvel, and R. I. Killey, "Spectrally-efficient single-sideband subcarrier-multiplexed quasi-Nyquist QPSK with direct detection," presented at the Eur. Conf. Opt. Commun., London, U.K., 2013, Paper Tu3C4.
[45] R. I. Killey, P. M. Watts, V. Mikhailov, M. Glick, and P. Bayvel, "Electronic dispersion compensation by signal predistortion using digital processing and a dual-drive Mach-Zehnder modulator," *IEEE Photon. Technol. Lett.*, vol. 17, no. 3, pp. 714–716, Mar. 2005.
[46] J. McNicol, M. O'Sullivan, K. Roberts, A. Comeau, D. McGhan, and L. Strawczynski, "Electrical domain compensation of optical dispersion [optical fibre communication applications]," presented at the Opt. Fiber Commun. Conf., Anaheim, CA, USA, 2005, Paper OThJ3.
[47] G. P. Agrawal, *Applications of Nonlinear Fiber Optics*, 3rd ed. San Francisco, CA, USA: Academic, 2010.
[48] C. E. Shannon, "A mathematical theory of communication," *Bell Syst. Technol. J.*, vol. 27, no. 3, pp. 379–423, 1948.
[49] N. Liu, C. Ju, and X. Chen, "Nonlinear ISI cancellation in VSSB Nyquist-SCM system with symbol pre-distortion," *Opt. Commun.*, vol. 338, pp. 492–495, 2015.

M. Sezer Erkılınç (S'11) received the B.Sc. degree in electrical and electronic engineering from Koç University, Istanbul, Turkey, in 2009, and the M.Sc. degree in electrical and electronic engineering from the Rochester Institute of Technology, Rochester, NY, USA, in 2011. He is currently working toward the Ph.D. degree at the Optical Networks Group, Department of Electronic and Electrical Engineering, University College London, London, U.K., since November 2011. He is currently investigating spectrally efficient modulation formats in direct detection links and simplified coherent receiver architectures for access and metropolitan/regional applications. He is a Graduate Student Member of the SPIE.

Zhe Li (S'15) received the B.Eng. degree in optical information science and technology from Jilin University, Jilin, China, in 2011. The following September, he joined University College London (UCL), London, U.K., to receive the M.Sc. degree in wireless and optical communications. In December 2013, he joined the Optical Networks Group at UCL as an M.Phil./Ph.D. candidate. Under the supervision of Dr. R. Killey, he is currently investigating spectrally efficient and low-cost optical communication systems with direct detection.

Stephan Pachnicke (M'09–SM'12) received the M.Sc. degree in information engineering from City University, London, U.K., in 2001, Dipl.Ing. and Dr. Ing. degrees in electrical engineering from TU Dortmund, Dortmund, Germany, in 2002 and 2005, respectively, and the Dipl.Wirt.Ing. degree in business administration from Fern Universitt, Hagen, Germany, in 2005. From 2007 to 2011, he was a Oberingenieur (Chief Engineer) with the Chair for High Frequency Technology, TU Dortmund. In January 2012, he finished his habilitation on optical transmission networks and since then he has been a Privatdozent (Adjunct Professor) with TU Dortmund. He is currently with ADVA Optical Networking SE with the Advanced Technology Group (CTO Office), Martinsried, Germany, where he is leading EU-funded research projects on next-generation optical access and fixed-mobile convergence. He is the Author or Coauthor of more than 80 scientific publications as well as Author of a book on *Fiber-Optic Transmission Networks* (New York, NY, USA: Springer, 2011). He is a Member of the VDE/ITG.

Helmut Griesser received the Dr. Ing. and Dipl. Ing. degrees in electrical engineering from the University of Ulm, Ulm, Germany. From 2002 to 2011, he was with Marconi and Ericsson working on high-speed fiber transmission. He is currently a Principal Engineer with the Advanced Technology Group, ADVA Optical Networking, Munich, Germany. His current research interests include signal processing, coding, modulation formats, and system design for optical fiber communication systems.

Benn C. Thomsen (M'06) received the B.Tech. degree in optoelectronics and the M.Sc. and Ph.D. degrees in physics from the University of Auckland, Auckland, New Zealand. His doctoral research included the development and characterization of short-optical pulse sources suitable for high-capacity optical communication systems. He then joined the Optoelectronics Research Centre, Southampton University, U.K., as a Research Fellow in 2002, where his research interests included ultrashort-optical pulse generation and characterization, optical packet switching based on optically coded labels, and all-optical pulse processing. He joined the Optical Networks Group, University College London (UCL), London, U.K., in 2004, where he was a Lecturer in 2007, and also held an EPSRC Advanced Fellowship from 2006 to 2011. He is currently a Senior Lecturer with UCL. His current research interests include optical transmission, physical-layer implementation of dynamic optical networking technology, and the development of high-capacity multimode fibre systems exploiting MIMO DSP.

Polina Bayvel received the B.Sc.(Eng.) and Ph.D. degrees in electronic and electrical engineering from the University of London, London, U.K., in 1986 and 1990, respectively. She was with the Fiber Optics Laboratory, General Physics Institute, Russian Academy of Sciences, Moscow, Russia, under the Royal Society Postdoctoral Exchange Fellowship. She was a Principal Systems Engineer with STC Submarine Systems Ltd., London, and with Nortel Networks, Harlow, U.K., and Ottawa, ON, Canada, where she was involved in the design and planning of optical fibre transmission networks. During 1994–2004, she held a Royal Society University Research Fellowship with University College London (UCL), London, U.K., and in 2002, she became a Chair in Optical Communications and Networks. She is currently the Head of the Optical Networks Group, UCL. She has authored or coauthored more than 350 refereed journal and conference papers. Her research interests include wavelength-routed optical networks, high-speed optical transmission, and the mitigation of fibre nonlinearities. She is a Fellow of the Royal Academy of Engineering, the Optical Society of America, the U.K. Institute of Physics, and the Institute of Engineering and Technology. She received the Royal Society Wolfson Research Merit Award (2007–2012), the 2013 IEEE Photonics Society Engineering Achievement Award, and the 2014 Royal Society Clifford Patterson Prize Lecture and Medal.

Robert I. Killey (M'00) received the B.Eng. degree in electronic and communications engineering from the University of Bristol, Bristol, U.K., in 1992, the M.Sc. degree from University College London (UCL), London, U.K., in 1994, and the Dr. Phil. degree from the University of Oxford, Oxford, U.K., in 1998. Following this, he joined the Optical Networks Group at UCL, where is currently a Reader in optical communications. His research interests include nonlinear fiber effects in WDM transmission systems, advanced modulation formats, and digital signal processing for optical communications. He is in the Technical Program Committees of ECOC and OFC conferences. He was a Member of the conference committees of the ACP, the OECC, and the IEEE LEOS Annual Meetings, and was General Cochair of the Signal Processing for Photonic Communications meeting at the OSA Advanced Photonics Congress. He was an Associate Editor of the IEEE/OSA *Journal of Optical Communications and Networking*.